

# THEORY OF GAS SENSOR MADE OF FIELD-EFFECT TRANSISTOR WITH NANOTUBES

V. M. Aroutiounian, B. V. Mnatsakanyan

Yerevan State University, Yerevan 0025, Armenia, e-mail: kisahar@ysu.am

Received 4 April, 2012

**Abstract**—We present a mathematical model of nanotube-based gas sensor. We consider a gas sensor as a back gate field-effect transistor with nanotube channel. A sensitivity of nanotube in gas media and back gate field-effect transistor current-voltage characteristics were modeled.

**Keywords:** gas sensor, nanotube sensitivity, field-effect transistor

## 1. Introduction

Improving of sensitivity, stability and selectivity as well as lower power consumption offered by commercially available sensors is necessary. One-dimensional semiconductor tubes (1DST) are very interesting and promising new materials for electronics, sensoric, etc. Carbon nanotubes (CNTs), silicon nanowires, etc. exhibit significantly better physical and chemical properties and response because of their nanoscale size. We hope that usual field-effect transistor (FETs) with a chemically sensing nanotube (nanowire) between the source and drain will be very promising chemical sensor. Interesting researches in the area of CNT-based gas sensors were carried out during the last decade, providing higher sensitivity, stability, and signal-to-noise ratio in gas sensing. Attempt to understand the influence of a gas on the electrical conductivity and response of a nanotube is reported in this paper.

## 2. Gas-Sensitive Nanotube

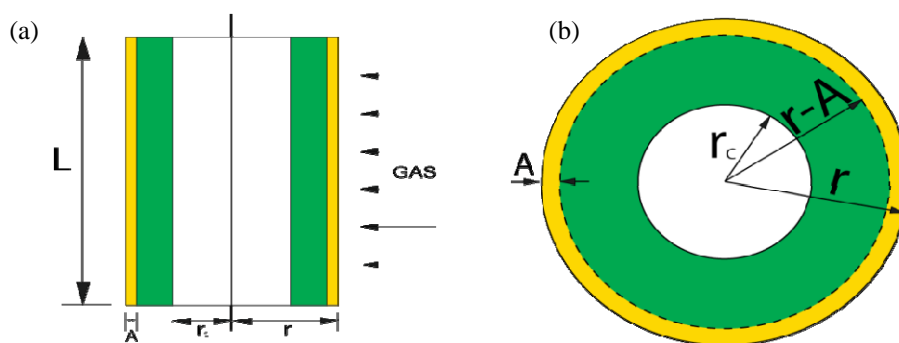


Fig. 1. a) Longitudinal section of 1DST; b) Cross section of 1DST.

Ohmic resistance  $R$  of the 1DST is equal to (see Fig. 1)

$$R = \rho \frac{L}{S'}, \quad (1)$$

where  $S' = \pi(r^2 - r_c^2)$ . The thickness layer  $A$  appears in a gas medium. Let the electron

concentration before placing of 1DST in gas medium be equal to  $n_0$ . In gas media, the concentration will change to  $n_A$ . In last case we have two resistances connected in parallel. The resistances of the outer layer  $R_0$  and the inner layer  $R_i$  are equal correspondingly to

$$R_i = \rho_0 \frac{L}{\pi[(r-A)^2 - r_c^2]}, \quad R_0 = \rho_A \times \frac{L}{\pi \times A^2}. \quad (2)$$

The sensitivity  $S$  is equal to

$$S = \frac{R_g}{R} = \frac{\rho_A}{\rho_0} \frac{r^2 - r_c^2}{A^2 + \frac{\rho_A}{\rho_0} [(r-A)^2 - r_c^2]}. \quad (3)$$

Calculation of the thickness  $A$  is carried out in cylindrical coordinates. As a result, we have following expression for  $A$ :

$$A = r \left( 1 - \sqrt{1 - \frac{2n_A}{n_0}} \right). \quad (4)$$

We have the expression for sensitivity

$$S = \left[ 1 + \frac{\eta^2 (\rho_0/\rho_A - 1)}{1 - r_c^2/r^2} \right]^{-1}, \quad (5)$$

where

$$\eta = 1 - \sqrt{1 - \frac{2n_A}{n_0}}. \quad (6)$$

Note that the non-equality

$$r_c/r < \sqrt{1 - 2n_A/n_0} \quad (7)$$

should be taken into account. This means that rather high level of changes in the concentration of electrons in the depletion layer  $A$  is necessary.

For the p-type 1DST  $n_A/n_0$  will be changed by  $p_A/p_0$ . Both versions ( $n$ - and  $p$ -type) are promising for the manufacture of gas sensors.

### 3. Back-gate CNFET

The physical structure of back-gate transistor is shown in Fig. 2. This model is based on the compact Spice model of CNFET [1], with some simplifications and modifications. The equivalent circuit model is shown in Fig. 3. We consider the current ( $I_{semi}$ ) between source(S) and drain (D) as [1]

$$I_{semi}(V_{DS}, V_{GS}) = 2 \sum_{m=1}^M \sum_{l=1}^L \left[ T_{LR} J_{m,l}(0, \Delta\Phi_B) \Big|_{+k} - T_{RL} J_{m,l}(V_{DS}, \Delta\Phi_B) \Big|_{-k} \right], \quad (8)$$

where  $V_{DS}$  and  $V_{GS}$  are potential differences,  $T_{LR}$  and  $T_{RL}$  are transmission probabilities [1],  $J_{m,l}$  is the current density [1].  $\Delta\Phi_B$  is the channel surface-potential change in response to the changes in the gate source/drain bias. In order to calculate  $\Delta\Phi_B$  we solve the charge conservation equations [1]

$$Q_{cap} = Q_{1DST},$$

$$Q_{1DST} = \frac{4e}{L_g} \sum_{m=1}^M \sum_{l=0}^L \left[ \frac{1}{1 + e^{(E_{m,l} - \Delta\Phi_B)/kT}} + \frac{1}{1 + e^{(E_{m,l} - \Delta\Phi_B + eV_{DS})/kT}} \right], \quad (9)$$

$$Q_{cap} = C_{ox} V_{GS} - \frac{C_{ox} \Delta\Phi_B}{e}. \quad (10)$$

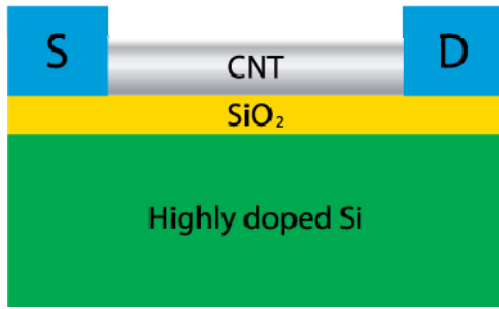


Fig. 2. The physical structure of back-gate FET.

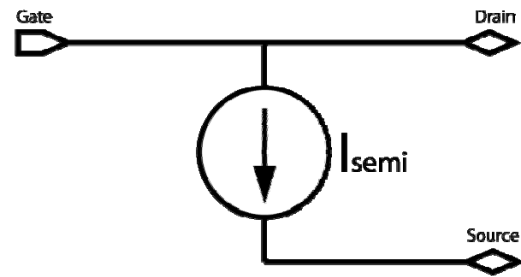


Fig. 3. The equivalent circuit model for a back-gate FET.

#### 4. Gas Sensor made with Nanotubes

In order to implement the final model gas sensor made of 1DST, we combine models of nanotube and back-gate FET. From formulas (3) and (8) we get

$$S = \frac{R_g}{R} = \frac{I}{I_g} = \frac{I_{semi}}{I_g}. \quad (11)$$

Therefore, the current ( $I_g$ ) for given charge concentration ratio and gate, source, drain bias will be

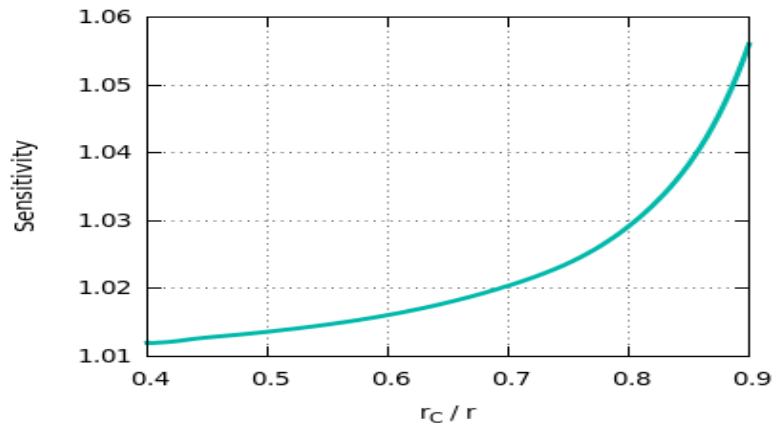
$$I_g = \frac{I_{semi}}{S}. \quad (12)$$

#### 5. Results and Discussion

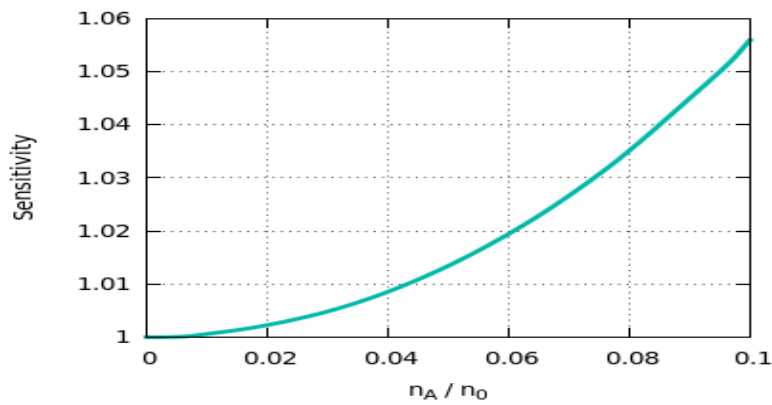
Fig. 4 shows the sensitivity of 1DST due to inner and outer radii ratio changes ( $n_A/n_0 = 0.1$ ). The maximum resistive change of 1DST due to gas medium is about 5.7% for this case. In general, we get a maximum 16% change of resistivity.

Fig. 5 shows the sensitivity of 1DST due to charge ratio changes ( $r_c/r = 0.9$ ). The maximum resistive change of 1DST due to gas medium is about 5.8% for this case. In general, we get a maximum 24% change of resistivity.

Fig. 6 shows the I-V characteristics change of gas sensor due to gas medium.



**Fig. 4.** The sensitivity of nanotube at  $n_A/n_0 = 0.1$ .



**Fig. 5.** The sensitivity of nanotube  $r_C/r = 0.9$ .

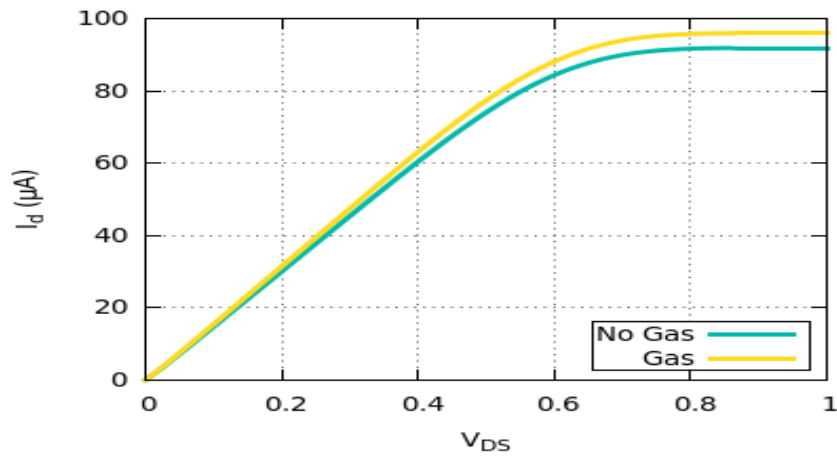


**Fig. 6.** The change of I-V characteristic of gas sensor due to gas medium.

## 6. Conclusion

We present mathematical model of gas sensor based on FET. In order to implement it we considered two models: 1DST model, the sensitivity of which depends on the charge ratio and outer and inner radii ratio, and simple back-gate FET model. Both models and final gas sensor model are mathematically described in Octave language (see Appendix).

## REFERENCES

1. **J.Deng, H.-S.P.Wong**, IEEE Trans. Electron. Devices, **54(12)**, 3195 (2007).

**Appendix: Mathematical model**

```

function k = k_m(m)
    global diameter;
    lambda = (6 .* m - 3 - (-1) .^ m) / 12;
    k = 2 * m * lambda / diameter;
endfunction
function k = k_l(l)
    global Lg;
    k = 2 * pi * l / Lg;
endfunction
function E_m_l = E_m_l(m, l)
    global a;
    global V_pi;
    E_m_l = sqrt(3) / 2 * a * V_pi * sqrt(k_m(m) .^ 2 + k_l(l) .^ 2);
endfunction
function f_FD = f_FD(E)
    global k;
    global T;
    f_FD = 1 ./ (1 + exp(E / (k * T)));
endfunction
function J_m_l = J_m_l(V_xs, delta_phi_B, m, l)
    global h;
    global a;
    global V_pi;
    global Lg;
    global k;
    global T;
    global q;
    t1 = 2 * q / h;
    t2 = sqrt(3) * a * pi * q * V_pi / Lg;
    t3 = k_l(l) / sqrt(k_m(m) .^ 2 + k_l(l) .^ 2);
    t4 = f_FD((E_m_l(m, l) + V_xs - delta_phi_B));
    J_m_l = t1 * t2 * t3 * t4;
endfunction
function I = I_semi(V_DS, V_GS, delta_phi_B, m, l)
    I = 0;
    for i = 1:m
        for j = 1:l
            I = I + 2 * (T_LR(V_DS, delta_phi_B, i, j) * J_m_l(0, delta_phi_B, i, j) - T_RL
(delta_phi_B, i, j) * J_m_l(V_DS, delta_phi_B, i, j));
        endfor
    endfor
endfunction
function D = D(E, m, l)
    global D_0;
    Eml = E_m_l(m, 0);
    if (E > Eml)
        D = D_0 * E / sqrt(E .^ 2 - Eml .^ 2);
    else
        D = 0;
    endif
endfunction
function f = d_phi_B(delta_phi_B)
    global C_ox;
    global V_GS;
    global V_FB;
    global q;
    global m;
    global l;
    global Lg;
    global k;
    global T;
    global V_DS;
    q_cap = C_ox * (V_GS - V_FB) - delta_phi_B * C_ox;

```

```

q_ = 0;
for i = 1:m
for j = 0:l
q_ = q_ + f_FD(E_m_l(m,l) - delta_phi_B) + f_FD(E_m_l(m,l) - delta_phi_B + V_DS);
endfor endfor
q_cnt = 4 * q * q_ / Lg;
f(1) = q_cnt - q_cap;
endfunction
function l_ap = l_ap(V_xs, delta_phi_B, m, l)
global lambda_ap;
global D_0;
global q;
E = E_m_l(m, l);
l_ap = lambda_ap * D_0 ./ (D(E, m, l) .* (1 - f_FD(E) - delta_phi_B + q .* V_xs));
endfunction
function l_op = l_op(V_xs, delta_phi_B, m, l)
global lambda_op;
global D_0;
global E_op;
global q;
E = E_m_l(m, l);
l_op = lambda_op * D_0 ./ (D(E, m, l) .* (1 - f_FD(E - E_op - delta_phi_B + q .* V_xs)));
endfunction
function l_eff = l_eff(V_xs, delta_phi_B, m, l)
lap = l_ap(V_xs, delta_phi_B, m, l);
lop = l_op(V_xs, delta_phi_B, m, l);
l_eff = (lap .* lop) ./ (lap + lop);
endfunction
function T_LR = T_LR(V_DS, delta_phi_B, m, l)
global Lg;
leff = l_eff(V_DS, delta_phi_B, m, l);
T_LR = leff / (leff + Lg);
endfunction
function T_RL = T_RL(delta_phi_B, m, l)
global Lg;
leff = l_eff(0, delta_phi_B, m, l);
T_RL = leff / (leff + Lg);
endfunction
global d = 0.144e-9;          # The carbon PI - PI bond distance
global a = sqrt(3) * d;      # The lattice constant
global diameter = 1.5e-9;    # Diameter of CNT
global Lg = 32e-9;          # Length of CNT
global V_pi = 3.033;         # PI - PI bond energy(ev)
global k = 8.617e-5;         # The Boltzmann constant
global T = 27 + 273;         # Temperature(Kelvin)
global lambda_ap = 500e-9;   # The optical phonon-scattering MFP
global lambda_op = 15e-9;    # The acoustic phonon-scattering MFP
global D_0 = 8 / (3 * pi * V_pi * d); # DOS
global E_op = 0.16;          # Threshold energy
global m = 3;                # Number of subbands
global l = 18;               # Number of substates
global h = 6.63e-34;         # Planck constant
global q = 1.6e-19;          # The electron's charge
global V_DS = 0.9;
global V_GS = 0.9;
global V_FB = 0;
global C_ox = 100e-16;
global delta_phi_B = 0;
for i = 1:1:20
V_DS = i / 20;
delta_phi_B = fsolve(@d_phi_B, 0)
oo(i) = I_semi(V_DS, V_GS, delta_phi_B, m, l);
endfor
x = 0.05:0.05:1;
plot(x, oo);
pause();

```